Bioorganic Chemistry 83 (2019) 198–204

Contents lists available at ScienceDirect

Bioorganic Chemistry

journal homepage: www.elsevier.com/locate/bioorg

4-Substituted benzenesulfonamides featuring cyclic imides moieties exhibit potent and isoform-selective carbonic anhydrase II/IX inhibition

Alaa A.-M. Abdel-Aziz[a,b,*], Adel S. El-Azab[a,c], Adel H. Ghiaty[c], Paola Gratteri[d], Claudiu T. Supuran[e], Alessio Nocentini[d,e,*]

[a] Department of Pharmaceutical Chemistry, College of Pharmacy, King Saud University, Riyadh 11451, Saudi Arabia
[b] Department of Medicinal Chemistry, Faculty of Pharmacy, Mansoura University, Mansoura 35516, Egypt
[c] Department of Organic Chemistry, Faculty of Pharmacy, Al-Azhar University, Cairo 11884, Egypt
[d] NEUROFARBA Department – Pharmaceutical and Nutraceutical Section, Laboratory of Molecular Modeling Cheminformatics & QSAR University of Florence, Via Ugo Schiff 6, 50019 Sesto Fiorentino, Florence, Italy
[e] NEUROFARBA Department – Pharmaceutical and Nutraceutical Section, University of Florence, Via Ugo Schiff 6, 50019 Sesto Fiorentino, Florence, Italy

ARTICLE INFO

Keywords:
Carbonic anhydrase
Inhibition
Heterocycle
Imide
Sulfonamide
Anti-glaucoma
Anti-tumor

ABSTRACT

The synthesis, characterization and biological evaluation of series of cyclic imides incorporating the 4-sulfamoylbenzamide scaffold (**16–29**) is disclosed. The compounds were designed by application of the "tail approach" to the aromatic sulfonamide scaffold and prepared by reacting the proper acid anhydride with 4-(hydrazinecarbonyl)benzenesulfonamide (**15**). Phtalimides and cyclic imides are biologically privileged scaffolds, endowed with versatile biological activity, such as an anti-proliferative action. The compounds were investigated for the inhibition of four human (h) isoforms of zinc enzyme carbonic anhydrase (CA, EC 4.2.1.1), and more specifically against the cytosolic hCA I and II and the transmembrane hCA IV and IX. Most screened sulfonamides exhibited great potency in inhibiting CA isoforms II, widely involved in glaucoma and other pathologies (K_Is in the range of 0.7–62.3 nM), and IX, that is a validated anti-tumor target (K_Is in the range of 3.0–50.9 nM), whereas interesting hydrophilicity-dependent inhibitory profiles were measured against isoform CA IV (K_Is in the range of 3.9–428.6 nM). *In silico* studies were carried out to assess the binding mode of selected derivatives to hCA II, IV and IX.

1. Introduction

Carbonic anhydrases (CAs, EC 4.2.1.1) consist of a cluster of zinc enzymes present throughout most living organisms and encoded by seven evolutionarily unrelated gene families: the α-, β-, γ-, δ-, ζ-, η and θ-CAs [1–3]. The CAs catalyze the reversible hydration of CO_2 into HCO_3 and protons by a metal hydroxide nucleophilic mechanism [1,2]. The 15 different α-CA isoforms identified in humans (h) differ by molecular features, oligomeric arrangement, cellular localization, distribution in organs and tissues, expression levels, kinetic properties and response to different classes of inhibitors. Some such isoforms are cytosolic (CA I, CA II, CA III, CA VII and CA XIII), others are membrane bound (CA IV, CA IX, CA XII, CA XIV and CA XV), two of them are mitochondrial (CA VA and CA VB), and one isozyme is secreted in saliva (CA VI) [2]. A wealth of human physiological-pathological processes exhibit abnormal levels or activities of these enzymes, making hCAs valuable targets for many pharmacological applications [1]. Inhibitors (CAIs) targeting hCA II are used as diuretics, in the management edema, as antiglaucoma agents, antiepileptic drugs, and also for the treatment of altitude sickness [1,2]. Nevertheless, the ubiquitous CA I and II are nowadays considered off-target for most current CAIs therapeutic applications, such as the anti-tumor or anti-inflammatory ones [4–8]. In such contexts, CA IV and CA IX stand out as the most interesting amongst hCAs in various pharmaceutical fields. CA IV is a drug target for glaucoma (together with CA II and XII), retinitis pigmentosa, stroke and rheumatoid arthritis [1,9,10]. CA IX, a transmembrane isoform, was shown to be implicated in diverse types of inflammation [8], but its main feature is to be overexpressed in many hypoxic tumors where it plays a role in cancer growth and metastases formation [4–7]. CA IX has become an attractive target for the design of antineoplastic therapies

* Corresponding authors at: Department of Pharmaceutical Chemistry, College of Pharmacy, King Saud University, Riyadh 11451, Saudi Arabia (A.A.-M. Abdel-Aziz). NEUROFARBA Department – Pharmaceutical and Nutraceutical Section, Laboratory of Molecular Modeling Cheminformatics & QSAR University of Florence, Via Ugo Schiff 6, 50019 Sesto Fiorentino, Florence, Italy (A. Nocentini).
E-mail addresses: almoenes@ksu.edu.sa (A.A.-M. Abdel-Aziz), alessio.nocentini@unifi.it (A. Nocentini).

https://doi.org/10.1016/j.bioorg.2018.10.037
Received 26 August 2018; Received in revised form 11 October 2018; Accepted 18 October 2018
Available online 19 October 2018
0045-2068/

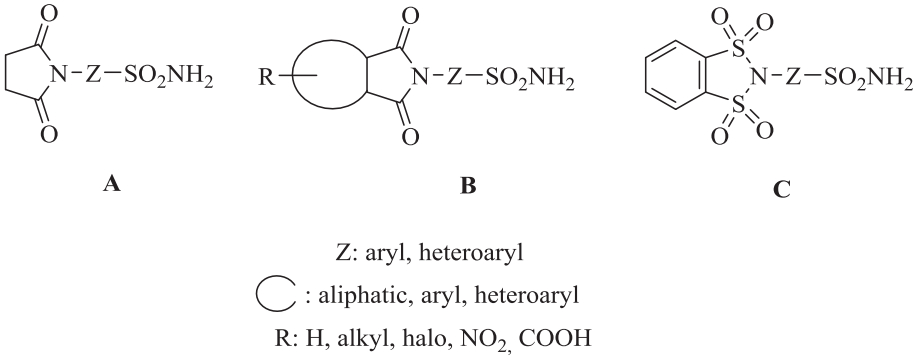

Fig. 1. Structures of previously reported sulfonamides incorporating cyclic imide moieties and ortho-benzenedisulfonimide.

[4]. To yield selective inhibition of some isoforms over others is a necessary endeavor to afford tools for the treatments of a plenty of pathologies showing minimum side effects [1].

Zinc binding group (ZBG) of the primary sulfonamide type are the first choice in the field of CAIs chemotypes [11]. In spite of their isoform-promiscuous efficacy a main approach is used for almost two decades to enable such scaffolds (mainly of the aromatic sulfonamide type) to selectively target precise hCAs, namely the "tail approach" [11–15]. In particular, the use of heterocyclic tails is the most exploited tool to seek for selectivity with sulfonamide-like inhibitors against the target hCAs [16–26]. Phthalimide and cyclic imide derivatives possess a variety pharmacological and biological activities, such as excellent anticancer profiles and inhibitory efficiency for several CA isoforms [16–26].

Compounds such as **A** and **B** (Fig. 1), incorporating phthalimide and/or cyclic imide moieties [19–22,27–30], were shown to possess potent inhibitory action against CA isoforms of relevant physiological functions (such as CA II, IV, VII, IX and XII). The similar ortho-benzenedisulfonimide derivatives **C** (Fig. 1), designed by considering the phthalimides **A**, **B** as lead compounds [27], were also shown to possess interesting inhibitory profiles against the tumor-associated isoforms CA IX.

Herein, synthesis and biological evaluation of novel 4-acetammidobenzenesulfonamides featuring cyclic imides moieties are proposed to go forward into the design of heterocyclic compounds of potential pharmacologic interest and study the effect of the incorporation of a hydrazide-like spacer between the cyclic imide and the main aromatic sulfonamide scaffold (Fig. 2). *In vitro* inhibition studies with compounds **16–29** are reported against hCA I, II, IV and IX. *In silico* studies were used to assess the binding mode of selected derivatives to hCA II, IV and IX.

2. Results and discussion

2.1. Chemistry

4-Sulfamoylbenzamide derivatives **16–29** were synthesized in 71–96% yields by heating the mixture of cyclic imides **1–14** and 4-(hydrazinecarbonyl)benzenesulfonamide (**15**) in glacial acetic acid in presence of anhydrous sodium acetate (Scheme 1) [19,20]. The structures of new synthesized compounds were confirmed by their elemental and spectral data. IR spectra of compounds **16–29** were used to verify

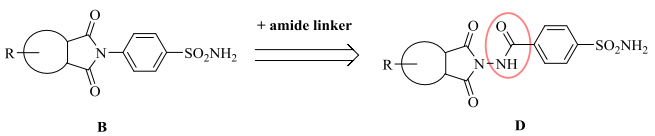

Fig. 2. Development of imides of hydrazide benzenesulfonamides (**D**) from **B**-like derivatives.

their structures through appearance of characteristic absorption bands due to (NH_2) and (NH) groups at 3413–3319 and 3279–3246 cm^{-1} as well as two bands for (SO_2) group at 1383–1312 and 1180–1136 cm^{-1} for 4-sulfamoylbenzamide moiety, in addition to carbonyl (C=O) groups at 1791–1715 and 1709–1684 cm^{-1} due to anhydride and amide moieties respectively. ^{1}H NMR spectra of compounds **16–29** were characterized by appearance of new singlet peaks of amide group (NH–C=O), as well as sulfamoyl group (SO_2NH_2) of 4-sulfamoylbenzamide moiety at 11.75–9.99 and 7.62–7.45 ppm respectively. Moreover, ^{13}C NMR spectra of compounds **16–29** showed new peak for amide group (NH–C=O) at 168.95–164.12 ppm, in addition to carbonyl group (CO) of aliphatic anhydride such as compounds **16** and **29** at 177.17–168.09 ppm, while carbonyl group (CO) of aromatic anhydride at 167.69–161.45 ppm.

2.2. Carbonic anhydrase inhibition

The CA inhibitory properties of imides **16–29** against human isoforms CA I, II, IV and IX were measured by a stopped flow CO_2 hydrase assay using acetazolamide (**AAZ**) as standard inhibitor [31]. The following structure–activity relationships (SAR) were gathered from the inhibition data reported in Table 1.

(i) The ubiquitous isoform CA I was moderately inhibited by cyclic imides **16–29** in the medium nanomolar to low micromolar range, with inhibition constants (K_Is) specifically spanning between 84.3 and 5167.3 nM. Incorporation of a *tert*-butyl moiety onto the outer phenyl ring increased the CA I inhibitory efficacy of **19** (K_I of 84.3 nM) three times respect to the aromatic unsubstituted analogue **17** (K_I of 297.8 nM). The polyhalogenated and/or bulky derivatives **24**, **25**, **27–29** possess a remarkably diminished inhibitory efficacy towards the ubiquitous isozyme (K_Is between 1098.6 and 5167.3 nM) compared to less hindered derivatives. A pyrazine core (**26**) in place of a benzene (**17**) do not substantially alter the inhibitory efficacy.

(ii) The cytosolic isoform CA II was undoubtedly the most inhibited among those screened (K_Is in the range of 0.7–128.1 nM). Again, derivative **19** stood out as best isoform inhibitor, showing a subnanomolar K_I of 0.7 nM. It may be observed that to incorporate more chlorine atoms on the outer aromatic ring did not significantly modify the inhibition potency of **24** (K_I of 5.0 nM) with respect to the unsubstituted **17** (K_I of 3.1 nM), whereas a stronger worsening was noticed by incorporation of bromine atoms (**25**, K_I of 62.3 nM). The bulky polychlorinated cyclic imide scaffold of **29** (K_I of 128.1 nM) arose as the least suitable to achieve CA inhibition, seen the almost ten-fold efficacy worsening of the derivative compared to the aliphatic analogue **16** (K_I of 17.8 nM).

(iii) The hCA IV inhibition profile with the compounds investigated here was quite interesting. Only a little number of derivatives, namely **20–22** and **28** had excellent inhibitory activity towards the

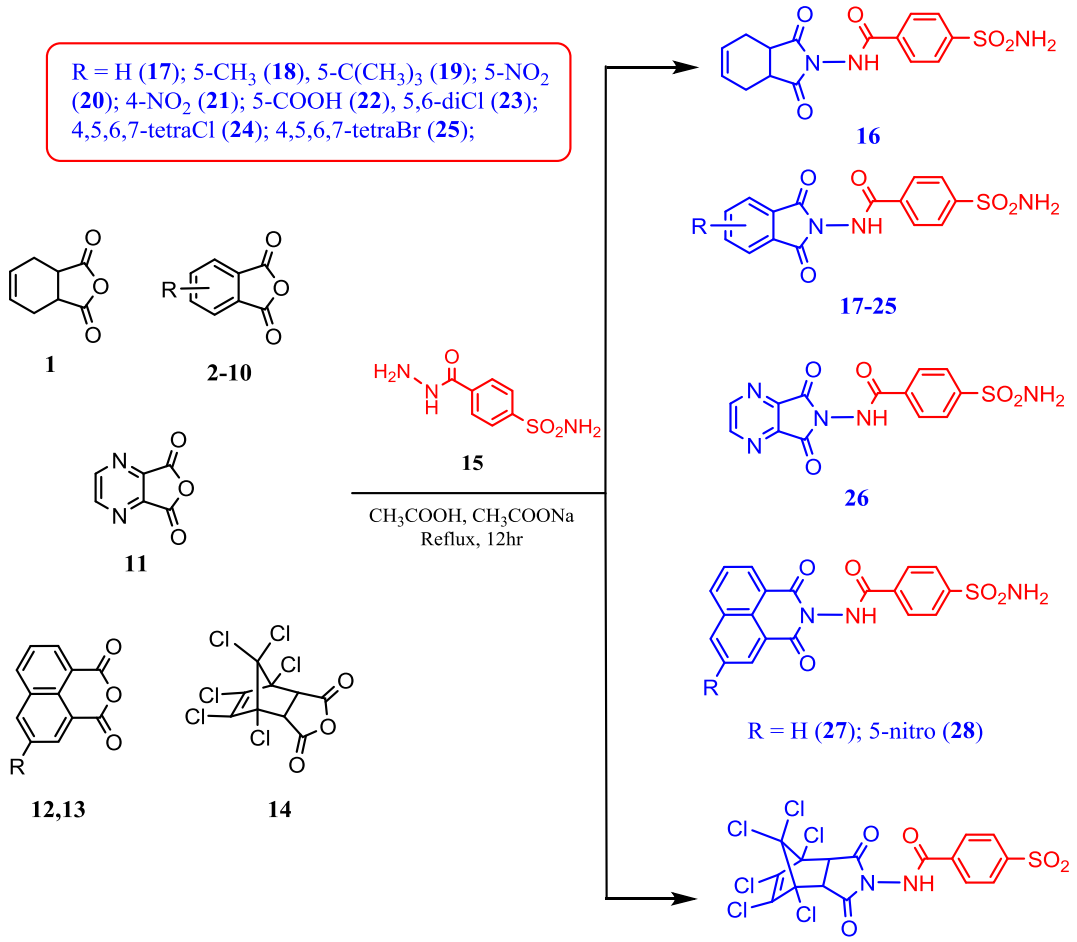

Scheme 1. Synthesis of cyclic imides incorporating 4-sulfamoylbenzamide **16–29.**

Table 1
Inhibition data of human CA isoforms hCA I, II, IV and IX with imides **16–29** and the standard sulfonamide inhibitor acetazolamide (**AAZ**) by a stopped flow CO_2 hydrase assay [31].

Cmpd	R	K_I (nM)*			
		CA I	CA II	CA IV	CA IX
16	–	191.6	17.8	351.3	113.6
17	-H	297.8	3.1	278.1	22.7
18	5-CH_3	176.8	9.1	263.9	18.6
19	5-$C(CH_3)_3$	84.3	0.7	206.3	7.7
20	5-NO_2	355.7	32.7	33.4	23.3
21	4-NO_2	119.9	51.6	17.8	50.9
22	5-COOH	354.9	61.4	3.9	31.0
23	5,6-diCl	736.2	20.2	199.8	26.4
24	4,5,6,7-tetraCl	1098.6	5.0	174.2	3.0
25	4,5,6,7-tetraBr	2389.0	62.3	106.0	8.4
26	–	161.7	50.8	150.3	192.2
27	-H	2622.6	7.7	428.6	28.8
28	5-NO_2	4507.3	20.6	82.3	22.4
29	–	5167.3	128.1	295.9	209.9
AAZ	–	250	12	74	25

* Mean from 3 different assays, by a stopped flow technique (errors were in the range of ± 10% of the reported values).

membrane-bound isozyme (K_Is of 33.4, 17.8, 3.9 and 82.3 nM, respectively). It should be noted that all such compounds bear hydrophilic moieties. In particular, the carboxylic acid **22** stood out indeed as the most potent CA IV inhibitor. Actually, CA IV possesses the most hydrophilic active site among hCAs and this justifies the obtained inhibitory profiles [32]. The pyrazine derivative **26** was oddly not among the strongest isoform inhibitors. Bulky and/or hydrophobic cyclic imide scaffolds did not confer to acetammido benzenesulfonamides marked CA IV inhibitory activity (K_Is between 106.0 and 428.6 nM).

(iv) The tumor-associated CA IX was also really sensitive to inhibition by hydrazide sulfonamide cyclic imide derivatives **16–29**. Inhibition constants were found to range in a low to medium nanomolar range (3.0–209.9 nM). The tetrachlorophenyl derivative **24** was the most potent inhibitor of the isoform, whereas the *tert*-butyl bearing **19** and the tetrabromophenyl compound **25** showed the second best and equipotent CA IX inhibition efficacy (7.7 and 8.4 nM, respectively) among those reported in Table 1.

Strangely, both the substitution of the benzene ring of **17** with a pyrazine (**26**) and the incorporation of the bulkiest cyclic imide scaffold as in **29** rather worsened the inhibitory efficacy with respect to most other substitutions (K_Is of 192.2 and 209.9 nM, respectively).

(v) The amide spacer between the cyclic imide portion and the main inhibitory scaffold does not lead to substantial inhibition improvements for the newly synthesized compounds in comparison to the previously reported imides [19–22]. Anyhow, few significant variations in the inhibition efficacy can be observed against CA II and IX depending on the substitution pattern on the aromatic imide core. For instance compound **19**, bearing a *t*-butyl moiety, acts 10 times better against CA II than the corresponding B-like analogue [22]. The nitro-derivative **20** shows a 5-fold more potent CA IX inhibition than its previously reported lead [22]. Conversely, CA I is remarkably less inhibited by **16–29** (high nanomolar-low

micromolar range) than **B**-like derivatives (low nanomolar range) [22].

(vi) Unfortunately, few compounds showed noteworthy target/off-target CAs selective action. Indeed, when the ubiquitous CA I was rather little inhibited by the reported sulfonamides, CA II turned out to be most affected one. Nevertheless, derivative **25** showed an eight-fold CA IX/II selective action as well as a CA IX/I selectivity index (SI) of 300. Interestingly, two compounds, **21** and **22,** exhibited a predominant activity towards CA IV for which selective inhibitors rather lack in literature. Indeed, **21** showed a three-fold CA IV/II selective action, whereas that of **22** reached a SI value of 15.

2.3. In silico studies

Selected compounds (**19**, **21**, **22**, **24**, **26**) were submitted to docking within CA isozymes II [13], IV [33] and IX [34] to rationalize the measured inhibition profiles. The docking solutions place the benzensulfonamide moiety of the derivatives deeply into the active site region of all isozymes, establishing two hydrogen bonds with a Thr residue (T199 in CA II/IV; T200 in CA IX). The sulfonamide negatively charged nitrogen atom directly coordinates the zinc ion and the phenyl ring is involved in several interactions with the hydrophobic inner portion of the cavities. The amide portion is not involved in any remarkable interaction within the three binding sites, likely justifying the almost analogue inhibition profiles of these compounds with the previously reported cyclic imides benzenesulfonamides (Fig. 3) [22]. In CA II, the phtalimide core accommodates in the hydrophic pocket formed by F131, L203 and V135 (Fig. 3A). As a result, compounds **19** and **24** that incorporate the most hydrophobic substituents stand out as the most active against CA II, with **19** even reaching a sub-nanomolar efficacy. In the active site of CA IV a hydrophilic region, rich of charged aminoacids replaces the typical hydrophobic half of hCAs. The 4-NO_2 and 5-COOH groups on the phtalimide aromatic core of **21** and **22** form a salt bridge with K206 (Fig. 3B), enhancing their CA IV inhibitory efficacy to a low nanomolar level. In CA IX, the cyclic imide moiety of these compounds lies in the hydrophobic region lined by L199, L134 and V130, establishing π-alkyl interactions with the residues side chains. The substitution of the benzene ring with a pyrazine one, in fact, lowers the CA IX inhibitory efficacy of **26** due to a diminished hydrophobic character of the aromatic portion (Fig. 3C).

3. Conclusions

The present work reported the synthesis, characterization and biological evaluation of a library of 4-acetammidobenzenesulfonamides featuring cyclic imides moieties. As a continuation of previous works on heterocyclic-tailed aromatic sulfonamide derivatives as CA inhibitors, the current study aimed to work out the effect of a different spacer (amide) between the cyclic imide portion and the main inhibitory scaffold (aromatic sulfonamide). The derivatives **16–29** were prepared by reacting different acid anhydrides with 4-(hydrazinecarbonyl)benzenesulfonamide. Many such compounds exhibited great potency in inhibiting CA isoform II, that although off-target in this study, is of interest to yield tools to treat several diseases, such as ocular pathologies (K_Is in the range of 0.7–62.3 nM). The target, tumor-associated CA IX was potently inhibited by a wealth of reported sulfonamides (K_Is in the range of 3.0–50.9 nM), revealing promising candidates for anticancer applications. Among these, a compound showed interesting target/off-target selectivity index paving the way to therapies devoid of most current isoforms-promiscuous action side effects. Although CA IV was not generally potently inhibited by **16–29**, three compounds (the most hydrophilic ones) exhibited a low nanomolar inhibitory efficacy. Two of them also reported a noteworthy CA IV/II selective activity that is quite difficult to find among benzenesulfonamide derivatives making them very interesting lead to design novel therapies in the treatment of retinitis pigmentosa, stroke and rheumatoid arthritis. *In silico* docking studies shed light on the binding modes of selected derivatives to CA II, IV and IX, aiding to rationalize the measured inhibitory profiles.

4. Experimental

4.1. Chemistry

Melting points (uncorrected) were recorded on Barnstead 9100 Electrothermal melting apparatus. IR spectra were recorded on a FT-IR Perkin-Elmer spectrometer. ^{1}H NMR and ^{13}C NMR were recorded in DMSO-d_6 and $CDCl_3$ on Bruker 500 and 125 MHz instrument, respectively, using TMS as internal standard (chemical shifts in δ ppm). Mass spectra were recorded on a Agilent 6320 Ion Trap mass spectrometers. Elemental analysis was carried out for C, H and N at the Research Centre of College of Pharmacy, King Saud University and the results are within ± 0.4% of the theoretical values. Compound **15** were prepared according to their reported procedure [35].

4.1.1. General procedure for the synthesis of cyclic imides incorporating 4-sulfamoylbenzamide 16–29 (Scheme 1)

A mixture of an appropriate cyclic imides **1–14** (5.0 mmol), 4-(hydrazinecarbonyl)benzenesulfonamide (**15**) (1.08 g, 5.0 mmol), and anhydrous sodium acetate (0.69 g, 5.0 mmol) in glacial acetic acid (20 mL) was heated under reflux for 12 h. After cooling the reaction mixture, the precipitate obtained was filtered, washed with water, dried and re-crystallised from acetic acid.

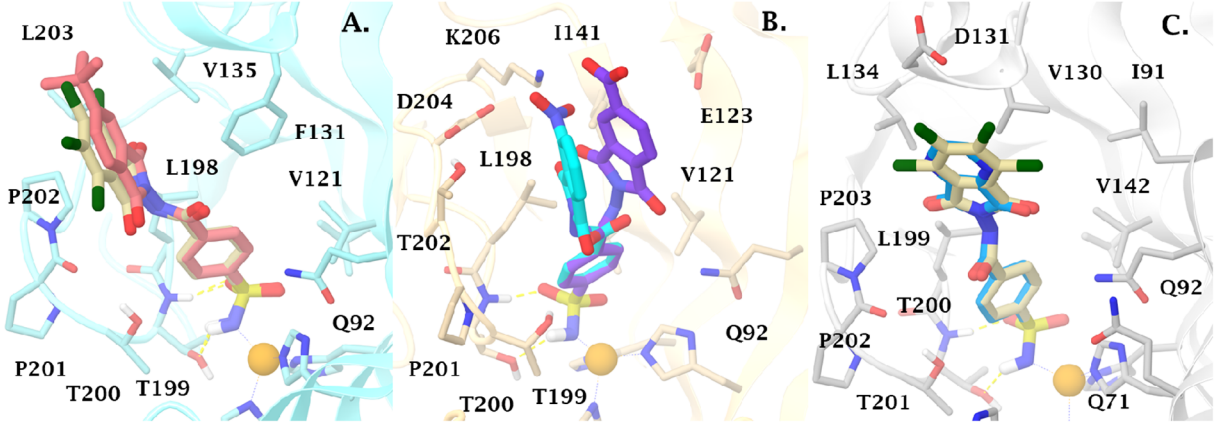

Fig. 3. Docking of (A) **19** and **24** to hCA II; (B) **21** and **22** to hCA IV; (C) **19** and **26** to hCA IX.

*4.1.1.1. N-(1,3-dioxo-1,3,3a,4,7,7a-hexahydro-2H-isoindol-2-yl)-4-sulfamoylbenzamide **(16)**.*

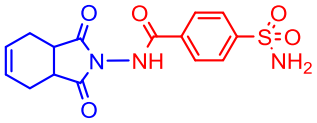

Yield, 91%; melting point (mp): 246–248 °C; IR (KBr, cm^{-1}) ν: 3351, 3261 (NH), 1798, 1743, 1709 (C═O), 1596, 1509 (C═C), 1245, 1099 (C–C), 1333, 1167 (O═S═O); ^{1}H NMR (500 MHz, DMSO-d_6): δ 11.41 11.41(0.5H), 11.28 (s, 0.5H), 8.06 (s, 2H), 7.99 (s, 2H), 7.57 (s, 2H), 5.95 (d, 2H, J = 6.5 Hz), 3.42 (s, 1H), 3.34 (s, 1H), 2.46–2.30 (m, 4H); ^{13}C NMR (125 MHz, DMSO-d_6): δ 23.18, 23.61, 37.28, 37.51, 126.49, 127.48, 128.25, 128.92, 134.16, 164.12, 177.17; C15H15N3O5S *m/z* (349).

*4.1.1.2. N-(1,3-dioxoisoindolin-2-yl)-4-sulfamoylbenzamide **(17)**.*

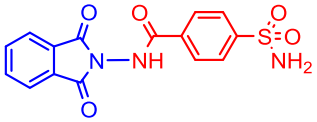

Yield, 93%; melting point (mp): 315–317 °C; IR (KBr, cm^{-1}) ν: 3344, 3246 (NH), 1736, 1701 (C═O), 1560, 1501 (C═C), 1276, 1092 (C–C), 1335, 1164 (O═S═O); ^{1}H NMR (500 MHz, DMSO-d_6): δ 11.58 (s, 1H), 8.16 (d, 2H, J = 6.5 Hz), 8.04 (d, 4H, J = 5.0 Hz), 7.98 (s, 2H), 7.61 (s, 2H); ^{13}C NMR (125 MHz, DMSO-d_6): δ 124.42, 126.59, 129.08, 129.92, 134.04, 135.94, 148.10, 165.09, 165.67; C15H11N3O5S: *m/z* (345).

*4.1.1.3. N-(5-methyl-1,3-dioxoisoindolin-2-yl)-4-sulfamoylbenzamide **(18)**.*

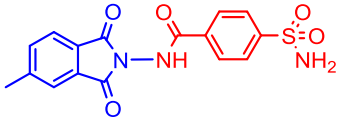

Yield, 89%; melting point (mp): 274–276 °C; IR (KBr, cm^{-1}) ν: 3319 (NH), 1770, 1735 (C═O), 1508 (C═C), 1273, 1091 (C–C), 1339, 1166 (O═S═O); ^{1}H NMR (500 MHz, DMSO-d_6): δ 11.53 (s, 1H), 8.14 (d, 2H, J = 6.0 Hz), 8.03 (d, 2H, J = 7.0 Hz), 7.91 (d, 1H, J = 6.0 Hz), 7.86 (s, 1H), 7.78 (d, 1H, J = 3.0 Hz), 7.61 (s, 2H), 2.54 (s, 3H); ^{13}C NMR (125 MHz, DMSO-d_6): δ 21.96, 124.34, 124.81, 126.57, 127.26, 129.04, 130.23, 134.06, 136.23, 147.11, 148.08, 165.04, 165.67, 165.81; C16H13N3O5S: *m/z* (359).

*4.1.1.4. N-(5-(tert-butyl)-1,3-dioxoisoindolin-2-yl)-4-sulfamoylbenzamide **(19)**.*

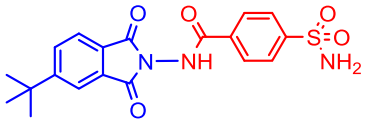

Yield, 94%; melting point (mp): 283–285 °C; IR (KBr, cm^{-1}) ν: 3345 (NH), 1786, 1734 (C═O), 1617, 1522 (C═C), 1275, 1103 (C–C), 1339, 1165 (O═S═O); ^{1}H NMR (700 MHz, DMSO-d_6): δ 11.58 (s, 1H), 8.15 (d, 2H, J = 7.0 Hz), 8.02 (q, 4H, J = 4.2 8.4 Hz), 7.96 (d, 1H, J = 9.1 Hz), 7.61 (s, 2H), 1.39 (s, 9H); ^{13}C NMR (176 MHz, DMSO-d_6): δ 31.17, 36.14, 121.27, 124.34, 126.56, 127.41, 129.06, 130.22, 132.77, 134.09, 148.05, 159.74, 165.04, 165.60, 165.93; C19H19N3O5S: *m/z* (401).

*4.1.1.5. N-(5-nitro-1,3-dioxoisoindolin-2-yl)-4-sulfamoylbenzamide **(20)**.*

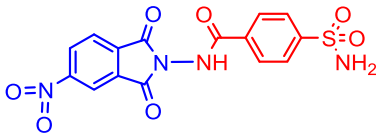

Yield, 75%; melting point (mp): 254–256 °C; ^{1}H NMR (500 MHz, DMSO-d_6): δ 10.59 (s, 1H), 8.34 (d, 2H, J = 7.0 Hz), 8.21 (s, 1H), 8.05 (d, 2H, J = 6.0 Hz), 7.98 (d, 2H, J = 6.5.0 Hz), 7.59 (s, 2H); ^{13}C NMR (125 MHz, DMSO-d_6): δ 123.12, 125.14, 125.99, 127.09, 128.00, 134.22, 135.80, 136.44, 137.78, 143.35, 146.61, 148.67, 164.77, 165.01; C15H10N4O7S: *m/z* (390).

*4.1.1.6. N-(4-nitro-1,3-dioxoisoindolin-2-yl)-4-sulfamoylbenzamide **(21)**.*

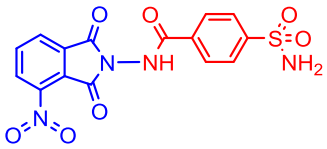

Yield, 77%; melting point (mp): 280–282 °C; IR (KBr, cm^{-1}) ν: 3372, 3269 (NH), 1742, 1684 (C═O), 1624, 1507 (C═C), 1270, 1095 (C–C), 1340, 1136 (O═S═O); ^{1}H NMR (700 MHz, DMSO-d_6): δ 9.99 (s, 1H), 8.08 (d, 1H, J = 7.7 Hz), 8.02 (d, 2H, J = 8.4 Hz), 7.91 (d, 2H, J = 7.0 Hz), 7.81 (t, 2H, J = 7.0 Hz), 7.45 (s, 2H); ^{13}C NMR (176 MHz, DMSO-d_6): δ 123.74, 125.57, 126.12, 127.98, 128.53, 134.66, 136.53, 137.73, 138.29, 139.41, 144.84, 146.19, 146.88, 164.70, 168.51; C15H10N4O7S: *m/z* (390).

*4.1.1.7. 1,3-dioxo-2-(4-sulfamoylbenzamido)isoindoline-5-carboxylic acid **(22)**.*

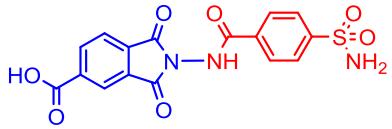

Yield, 71%; melting point (mp): 344–346 °C; ^{1}H NMR (700 MHz, DMSO-d_6): δ 13.11 (s, 1H), 10.05 (s, 1H), 8.32 (1, 1H), 8.19 (d, 2H, J = 7.7 Hz), 8.00 (d, 2H, J = 7.7 Hz), 7.94 (d, 2H, J = 7.7 Hz), 7.58 (s, 2H); ^{13}C NMR (176 MHz, DMSO-d_6): δ 123.52, 124.10, 126.40, 129.07, 129.70, 130.21, 135.81, 147.54, 147.71, 167.69, 168.94, 173.37; C16H11N3O7S: *m/z* (389).

*4.1.1.8. N-(5,6-dichloro-1,3-dioxoisoindolin-2-yl)-4-sulfamoylbenzamide **(23)**.*

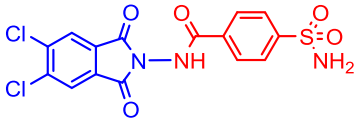

Yield, 91%; melting point (mp): 233–235 °C; IR (KBr, cm^{-1}) ν: 3337 (NH), 1734, 1686 (C═O), 1627, 1508 (C═C), 1291, 1092 (C–C), 1330, 1160 (O═S═O); ^{1}H NMR (500 MHz, DMSO-d_6): δ 11.68 (s, 1H), 8.38 (s, 2H), 8.14 (d, 2H, J = 8.0 Hz), 8.02 (d, 2H, J = 8.0 Hz), 7.60 (s, 2H); ^{13}C NMR (125 MHz, DMSO-d_6): δ 126.28, 126.57, 126.74, 128.78, 129.12, 129.72, 138.94, 148.16, 163.94, 165.05; C15H9Cl2N3O5S: *m/z* (414).

*4.1.1.9. 4-sulfamoyl-N-(4,5,6,7-tetrachloro-1,3-dioxoisoindolin-2-yl) benzamide **(24)**.*

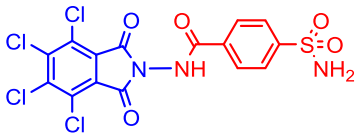

Yield, 96%; melting point (mp): 335–337 °C; IR (KBr, cm^{-1}) ν: 3266 (NH), 1783, 1715 (C=O), 1598, 1508 (C=C), 1207, 1130 (C–C), 1367, 1161 (O=S=O); ^{1}H NMR (500 MHz, DMSO-d_6): δ 10.26 (s, 1H), 8.14 (s, 2H), 8.03 (d, 2H, J = 6.0 Hz), 7.60 (s, 2H); ^{13}C NMR (125 MHz, DMSO-d_6): δ 126.58, 126.65, 129.17, 129.52, 139.84, 148.18, 161.35, 165.10; C15H7Cl4N3O5S: m/z (483).

*4.1.1.10. 4-sulfamoyl-N-(4,5,6,7-tetrabromo-1,3-dioxoisoindolin-2-yl) benzamide (**25**).*

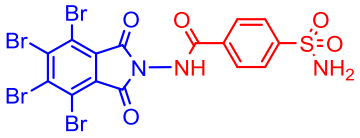

Yield, 95%; melting point (mp): 346–348 °C; IR (KBr, cm^{-1}) ν: 3374, 3270 (NH), 1785, 1742 (C=O), 1498 (C=C), 1270, 1095 (C–C), 1340, 1180 (O=S=O); ^{1}H NMR (500 MHz, DMSO-d_6): δ 11.72 (s, 1H), 8.15 (d, 2H, J = 7.0 Hz), 8.03 (d, 2H, J = 6.0 Hz), 7.60 (s, 2H); ^{13}C NMR (125 MHz, DMSO-d_6): δ 121.98, 126.60, 129.17, 129.43, 133.83, 138.11, 148.18, 161.72, 165.05; C15H7Br4N3O5S: m/z (660).

*4.1.1.11. N-(5,7-dioxo-5,7-dihydro-6H-pyrrolo[3,4-b]pyrazin-6-yl)-4-sulfamoylbenzamide (**26**).*

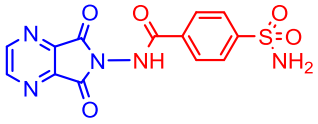

Yield, 80%; melting point (mp): 215–217 °C; IR (KBr, cm^{-1}) ν: 3323 (NH), 1772, 1721 (C=O), 1604, 1508 (C=C), 1269, 1124 (C–C), 1368, 1162 (O=S=O); ^{1}H NMR (700 MHz, DMSO-d_6): δ 10.52 (s, 1H), 9.98 (s, 2H), 8.02 (d, 2H, J = 7.7 Hz), 7.94 (d, 2H, J = 7.7 Hz), 7.54 (s, 2H); ^{13}C NMR (176 MHz, DMSO-d_6): δ 126.24, 126.33, 127.20, 128.61, 135.88, 147.20, 164.99, 168.95; C13H9N5O5S: m/z (347).

*4.1.1.12. N-(1,3-dioxo-1H-benzo[de]isoquinolin-2(3H)-yl)-4-sulfamoylbenzamide (**27**).*

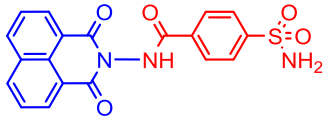

Yield, 89%; melting point (mp): 361–363 °C; IR (KBr, cm^{-1}) ν: 3413 (NH), 1774, 1700 (C=O), 1593, 1515 (C=C), 1289, 1121 (C–C), 1312, 1147 (O=S=O); ^{1}H NMR (500 MHz, DMSO-d_6): δ 11.59 (s, 1H), 8.59–8.54 (m, 4H), 8.20 (d, 2H, J = 8.0 Hz), 8.06 (d, 2H, J = 8.0 Hz), 7.95–7.92 (m, 2H), 7.62 (s, 2H); ^{13}C NMR (125 MHz, DMSO-d_6): δ 121.98, 126.55, 127.67, 127.99, 129.01, 132.01, 132.17, 134.94, 135.86, 147.83, 162.16, 164.85; C19H13N3O5S: m/z (395).

*4.1.1.13. N-(5-nitro-1,3-dioxo-1H-benzo[de]isoquinolin-2(3H)-yl)-4-sulfamoylbenzamide (**28**).*

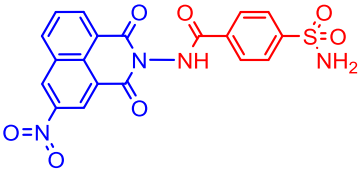

Yield, 92%; melting point (mp): 287–289 °C; IR (KBr, cm^{-1}) ν: 3371, 3263 (NH), 1777, 1731 (C=O), 1612, 1507 (C=C), 1269, 1088 (C–C), 1383, 1166 (O=S=O); ^{1}H NMR (500 MHz, DMSO-d_6): δ 11.72 (s, 1H), 9.57 (s, 1H), 9.04 (s, 1H), 8.87 (d, 1H, J = 8.0 Hz), 8.76 (t, 1H, J = 7.0 Hz), 8.19 (d, 2H, J = 8.5 Hz), 8.12 (t, 1H, J = 8.0 Hz), 8.05 (t, 2H, J = 8.5 Hz), 7.61 (s, 2H); ^{13}C NMR (125 MHz, DMSO-d_6): δ 122.40, 123.80, 124.49, 126.55, 129.08, 129.82, 129.94, 131.19, 131.65, 134.73, 135.37, 137.84, 146.40, 147.91, 161.09, 161.45, 164.88; C19H12N4O7S: m/z (440).

*4.1.1.14. N-(4,5,6,7,8,8-hexachloro-1,3-dioxo-1,3,3a,4,7,7a-hexahydro-2H-4,7-methanoisoindol-2-yl)-4-sulfamoylbenzamide (**29**).*

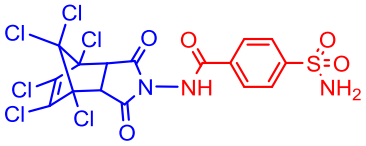

Yield, 91%; melting point (mp): 302–304 °C; IR (KBr, cm^{-1}) ν: 3346 (NH), 1772, 1721 (C=O), 1604, 1508 (C=C), 1269, 1124 (C–C), 1368, 1162 (O=S=O); ^{1}H NMR (700 MHz, DMSO-d_6): δ 11.75 (s, 0.32H),; 11.49 (s, 0.68H), 8.06 (d, 2H, J = 7.7 Hz), 7.99 (t, 2H, J = 8.4 Hz), 7.59 (s, 2H); 4.45 (s, 0.6H), 4.41 (s, 1.4H); ^{13}C NMR (176 MHz, DMSO-d_6): δ 50.35, 79.16, 79.41, 104.93, 126.48, 129.14, 129.20, 131.32, 133.88, 148.02, 168.09; C16H9Cl6N3O5S: m/z (568).

4.2. Carbonic anhydrase inhibition

An Applied Photophysics stopped-flow instrument has been used for assaying the CA catalyzed CO_2 hydration activity [31]. Phenol red (at a concentration of 0.2 mM) has been used as indicator, working at the absorbance maximum of 557 nm, with 20 mMHepes (pH 7.5) as buffer, and 20 mM Na_2SO_4 (for maintaining constant the ionic strength), following the initial rates of the CA-catalyzed CO_2 hydration reaction for a period of 10–100 s. The CO_2 concentrations ranged from 1.7 to 17 mM for the determination of the kinetic parameters and inhibition constants. For each inhibitor at least six traces of the initial 5–10% of the reaction have been used for determining the initial velocity. The uncatalyzed rates were determined in the same manner and subtracted from the total observed rates. Stock solutions of inhibitor (0.1 mM) were prepared in distilled-deionized water and dilutions up to 0.01 nM were done thereafter with the assay buffer. Inhibitor and enzyme solutions were preincubated together for 15 min at room temperature prior to assay, in order to allow for the formation of the E-I complex. The inhibition constants were obtained by non-linear least-squares methods using PRISM 3 and the Cheng–Prusoff equation, as reported earlier [36,37], and represent the mean from at least three different determinations. All CA isoforms were recombinant ones obtained in-house as reported earlier [34,38].

4.2.1. In silico studies

5LJT [13], 1ZNC [33] and 5FL4 [34] crystal structures was prepared according to the Protein Preparation module in Maestro - Schrödinger suite, assigning bond orders, adding hydrogens, deleting water molecules, and optimizing H-bonding networks [39]. Finally, energy minimization with a root mean square deviation (RMSD) value of 0.30 was applied using an Optimized Potentials for Liquid Simulation (OPLS3) force field. 3D ligand structures were prepared by Maestro [39] and evaluated for their ionization states at pH 7.4 ± 0.5 with Epik [39]. OPLS3 force field in Macromodel [39] was used for energy minimization for a maximum number of 2500 conjugate gradient iteration and setting a convergence criterion of 0.05 kcal $mol^{-1}Å^{-1}$. The docking grid was generated using Glide [39] with default settings, with the center located on the center of mass of the cocrystallized ligand. Ligands were docked employing Glide standard precision mode (SP) and OPLS3 FF retaining the best 5 poses of each molecule as output. The

top ranked binding pose of each compound was then analysed in terms of coordination, hydrogen bond interactions and hydrophobic contacts.

Acknowledgments

The authors extend their appreciation to the Deanship of Scientific Research at King Saud University for funding the work through the research group project No. RGP-163. Ente Cassa di Risparmio di Firenze, Italy, is gratefully acknowledged for a grant to A.N (ECR 2016.0774).

Appendix A. Supplementary material

Supplementary data to this article can be found online at https://doi.org/10.1016/j.bioorg.2018.10.037.

References

[1] C.T. Supuran, Carbonic anhydrases: novel therapeutic applications for inhibitors and activators, Nat. Rev. Drug Discovery 7 (2008) 168–181.
[2] (a) V. Alterio, A. Di Fiore, K. D'Ambrosio, C.T. Supuran, G. De Simone, Multiple binding modes of inhibitors to carbonic anhydrases: how to design specific drugs targeting 15 different isoforms? Chem. Rev. 112 (2012) 4421–4468;
(b) S. Del Prete, D. Vullo, G.M. Fisher, K.T. Andrews, S. Poulsen, C. Capasso, C.T. Supuran, Discovery of a new family of carbonic anhydrases in the malaria pathogen *Plasmodium falciparum*. The η-carbonic anhydrases, Bioorg. Med. Chem. Lett. 18 (2014) 4389–4396.
[3] S. Kikutani, K. Nakajima, C. Nagasato, Y. Tsuji, A. Miyatake, Y. Matsuda, Thylakoid luminal theta-carbonic anhydrase critical for growth and photosynthesis in the marine diatom phaeodactylum tricornutum, Proc. Natl. Acad. Sci. 113 (2016) 9828–9833.
[4] (a) C.T. Neri, Supuran, interfering with pH regulation in tumours as a therapeutic strategy, Nat. Rev. Drug Discov. 10 (2011) 767–777;
(b) C.T. Supuran, Carbonic anhydrase inhibition and the management of hypoxic tumors, Metabolites 7 (2017) E48.
[5] G. De Simone, C.T. Supuran, Carbonic anhydrase IX: biochemical and crystallographic characterization of a novel antitumor target, Biochim. Biophys. Acta 2010 (1804) 404–409.
[6] J. Pastorek, S. Pastorekova, Hypoxia-induced carbonic anhydrase IX as a target for cancer therapy: from biology to clinical use, Semin. Cancer Biol. 31 (2015) 52–64.
[7] A. Nocentini, C.T. Supuran, Carbonic anhydrase inhibitors as antitumor/antimetastatic agents: a patent review (2008–2018), Expert Opin. Ther. Pat. (2018), https://doi.org/10.1080/13543776.2018.1508453.
[8] F. Margheri, M. Ceruso, F. Carta, A. Laurenzana, L. Maggi, S. Lazzeri, G. Simonini, F. Annunziato, M. Del Rosso, C.T. Supuran, R. Cimaz, Overexpression of the transmembrane carbonic anhydrase isoforms IX and XII in the inflamed synovium, J. Enzyme Inhib. Med. Chem. 31 (2016) 60–63.
[9] H. Matsui, M. Murakami, G.C. Wynns, C.W. Conroy, A. Mead, T.H. Maren, M.L. Sears, Membrane carbonic anhydrase (IV) and ciliary epithelium. Carbonic anhydrase activity is present in the basolateral membranes of the non-pigmented ciliary epithelium of rabbit eyes, Exp. Eye Res. 62 (62) (1996) 409–417.
[10] Y. Tang, H. Xu, Du, L. Lit, W. Walker, A. Lu, R. Ran, J.P. Gregg, M. Reilly, A. Pancioli, J. Khoury, L.R. Sauerbeck, J.A. Carrozzella, J. Spilker, J. Clark, K.R. Wagner, E.C. Jauch, D.J. Chang, P. Verro, J.P. Broderick, F.R. Sharp, Gene expression in blood changes rapidly in neutrophils and monocytes after ischemic stroke in humans: a microarray study, J. Cereb. Blood Flow Metab. 26 1089 (2006) 1102.
[11] C.T. Supuran, How many carbonic anhydrase inhibition mechanisms exist? J. Enzyme Inhib. Med. Chem. 31 (2016) 345–360.
[12] A. Scozzafava, L. Menabuoni, F. Mincione, F. Briganti, G. Mincione, C.T. Supuran, Carbonic anhydrase inhibitors. Synthesis of water-soluble, topically effective, intraocular pressure-lowering aromatic/heterocyclic sulfonamides containing cationic or anionic moieties: is the tail more important than the ring? J. Med. Chem. 42 (1999) 2641–2650.
[13] A. Nocentini, M. Ferraroni, F. Carta, M. Ceruso, P. Gratteri, C. Lanzi, E. Masini, C.T. Supuran, Benzenesulfonamides incorporating flexible triazole moieties are highly effective carbonic anhydrase inhibitors: synthesis and kinetic, crystallographic, computational, and intraocular pressure lowering investigations, J. Med. Chem. 59 (2016) 10692–10704.
[14] A. Nocentini, S. Bua, C.L. Lomelino, R. McKenna, M. Menicatti, G. Bartolucci, B. Tenci, L. Di Cesare Mannelli, C. Ghelardini, P. Gratteri, C.T. Supuran, Discovery of new sulfonamide carbonic anhydrase IX inhibitors incorporating nitrogenous bases, ACS Med. Chem. Lett. 8 (2017) 1314–1319.
[15] D. Vullo, S. Del Prete, A. Nocentini, S.M. Osman, Z. AlOthman, C. Capasso, M. Bozdag, F. Carta, P. Gratteri, C.T. Supuran, Dithiocarbamates effectively inhibit the β-carbonic anhydrase from the dandruff-producing fungus *Malassezia globosa*, Bioorg. Med. Chem. 25 (2017) 1260–1265.
[16] W.M. Eldehna, M.F. Abo-Ashour, A. Nocentini, P. Gratteri, I.H. Eissa, M. Fares, O.E. Ismael, H.A. Ghabbour, M.M. Elaasser, H.A. Abdel-Aziz, C.T. Supuran, Novel 4/3-((4-oxo-5-(2-oxoindolin-3-ylidene)thiazolidin-2-ylidene)amino) benzenesulfonamides: synthesis, carbonic anhydrase inhibitory activity, anticancer activity and molecular modelling studies, Eur. J. Med. Chem. 139 (2017) 250–262.
[17] A.A.-M. Abdel-Aziz, K.E.H. ElTahir, Y.A. Asiri, Synthesis, anti-inflammatory activity and COX-1/COX-2 inhibition of novel substituted cyclic imides. Part 1: molecular docking study, Eur. J. Med. Chem. 46 (2011) 1648–1655.
[18] A.A.-M. Abdel-Aziz, Novel and versatile methodology for synthesis of cyclic imides and evaluation of their cytotoxic, DNA binding, apoptotic inducing activities and molecular modeling study Eur, J. Med. Chem. 42 (2007) 612–626.
[19] M.A. Mohamed, A.A.-M. Abdel-Aziz, H.M. Sakr, A.S. El-Azab, S. Bua, C.T. Supuran, Synthesis and human/bacterial carbonic anhydrase inhibition with a series of sulfonamides incorporating phthalimido moieties, Bioorg. Med. Chem. 25 (2017) 2524–2529.
[20] A.S. El-Azab, A.A.-M. Abdel-Aziz, R.R. Ayyad, M. Ceruso, C.T. Supuran, Inhibition of carbonic anhydrase isoforms I, II, IV, VII and XII with carboxylates and sulfonamides incorporating phthalimidephthalic anhydride scaffolds, Bioorg. Med. Chem. 24 (2016) 20–25.
[21] A.M. Alanazi, A.S. El-Azab, I.A. Al-Suwaidan, K.E.H. ElTahir, Y.A. Asiri, N.I. Abdel-Aziz, A.A.-M. Abdel-Aziz, Structure-based design of phthalimide derivatives as potential cyclooxygenase-2 (COX-2) inhibitors: anti-inflammatory and analgesic activities, Eur. J. Med. Chem 92 (2015) 115–123.
[22] A.A.-M. Abdel-Aziz, A.S. El-Azab, M. Ceruso, C.T. Supuran, Carbonic anhydrase inhibitory activity of sulfonamides and carboxylic acids incorporating cyclic imide scaffolds, Bioorg. Med. Chem. Lett. 24 (2014) 5185–5189.
[23] I.A. Al-Suwaidan, A.M. Alanazi, A.S. El-Azab, A.A.-M. Abdel-Aziz, Molecular design, synthesis and biological evaluation of cyclic imides bearing benzenesulfonamide fragment as potential COX-2 inhibitors, Bioorg. Med. Chem. Lett. 23 (2013) 2601–2605.
[24] A.S. El-Azab, A.M. Alanazi, N.I. Abdel-Aziz, I.A. Al-Suwaidan, M.A.A. El-Sayed, M.A. ElSherbeny, A.A.-M. Abdel-Aziz, Synthesis, molecular modeling study, preliminary antibacterial, and antitumore valuation of N-substituted naphthalimides and their structural analogues, Med. Chem. Res. 22 (2013) 2360–2375.
[25] A.A.-M. Abdel-Aziz, A.S. El-Azab, S.M. Attia, A.M. Al-Obaid, H.I. Al-Omar El-Subbagh, Synthesis and biological evaluation of some novel cyclic-imides as hypoglycaemic, anti-hyperlipidemic agents, Eur. J. Med. Chem. 46 (2011) 4324–4329.
[26] A.S. El-Azab, S.G. Abdel-Hamide, M.M. Sayed-Ahmed, G.S. Hassan, T.M. El-Hadiyah, O.A. Al-Shabanah, O.A. Al-Deeb, H.I. El-Subbagh, Novel 4(3H)-quinazolinone analogs: synthesis and anticonvulsant activity, Med. Chem. Res 22 (2013) 2815–2827.
[27] A. Scozzafava, F. Mincione, L. Menabuoni, C.T. Supuran, Drug Des. Discov. 17 (2001) 337.
[28] K.K. Sethi, D. Vullo, S.M. Verma, M. Tanç, F. Carta, C.T. Supuran, Bioorg. Med. Chem. 21 (2013) 5973.
[29] K.K. Sethi, S.M. Verma, M. Tanç, G. Purper, G. Calafato, F. Carta, C.T. Supuran, Bioorg. Med. Chem. 22 (2014) 1586.
[30] A.A. Abdel-Aziz, A.S. El-Azab, M.A. Abu El-Enin, A.A. Almehizia, C.T. Supuran, A. Nocentini, Synthesis of novel isoindoline-1,3-dione-based oximes and benzenesulfonamide hydrazones as selective inhibitors of the tumor-associated carbonic anhydrase IX, Bioorg Chem. 80 (2018) 706–713.
[31] R.G. Khalifah, The carbon dioxide hydration activity of carbonic anhydrase, J. Biol. Chem. 246 (1971) 2561–2573.
[32] N. Chiaramonte, S. Bua, M. Ferraroni, A. Nocentini, A. Bonardi, G. Bartolucci, M. Durante, L. Lucarini, D. Chiapponi, S. Dei, D. Manetti, E. Teodori, P. Gratteri, E. Masini, C.T. Supuran, M.R. Romanelli, 2-Benzylpiperazine: a new scaffold for potent human carbonic anhydrase inhibitors. Synthesis, enzyme inhibition, enantioselectivity, computational and crystallographic studies and in vivo activity for a new class of intraocular pressure lowering agents, Eur. J. Med. Chem. 10 (151) (2018 May) 363–375.
[33] T. Stams, S.K. Nair, T. Okuyama, A. Waheed, W.S. Sly, D.W. Christianson, Crystal structure of the secretory form of membrane-associated human carbonic anhydrase IV at 2.8-A resolution, Proc. Natl. Acad. Sci. USA 93 (1996) 13589–13594.
[34] J. Leitans, A. Kazaks, A. Balode, J. Ivanova, R. Zalubovskis, C.T. Supuran, K. Tars, Efficient Expression and crystallization system of cancer-associated carbonic anhydrase isoform IX, J. Med. Chem. 58 (2015) 9004–9009.
[35] Y1. Takaoka, H. Tsutsumi, N. Kasagi, E. Nakata, I. Hamachi, One-pot and sequential organic chemistry on an enzyme surface to tether a fluorescent probe at the proximity of the active site with restoring enzyme activity, J. Am. Chem. Soc. 128 (10) (2006) 3273–3280 Mar15.
[36] A. Nocentini, R. Cadoni, P. Dumy, C.T. Supuran, J.Y. Winum, Carbonic anhydrases from *Trypanosoma cruzi* and *Leishmania donovani* chagasi are inhibited by benzoxaboroles, J. Enzyme Inhib. Med. Chem. 33 (1) (2018) 286–289.
[37] H.S. Ibrahim, H.A. Allam, W.R. Mahmoud, A. Bonardi, A. Nocentini, P. Gratteri, E.S. Ibrahim, H.A. Abdel-Aziz, C.T. Supuran, Dual-tail arylsulfone-based benzenesulfonamides differently match the hydrophobic and hydrophilic halves of human carbonic anhydrases active sites: selective inhibitors for the tumor-associated hCA IX isoform, Eur. J. Med. Chem. 152 (2018) 1–9.
[38] A. Nocentini, D. Moi, G. Balboni, S. Salvadori, V. Onnis, C.T. Supuran, Synthesis and biological evaluation of novel pyrazoline-based aromatic sulfamates with potent carbonic anhydrase isoforms II, IV and IX inhibitory efficacy, Bioorg Chem. 77 (2018) 633–639.
[39] Schrodinger Suite Release 2016-1, Schrodinger, LLC, New York, NY, 2016. (a) Maestro v.10.5; (b) Epik v.3.5; (c) Impact v.7.0; (d) Prime v.4.3; (e) Macromodel v. 11.1; (f) Glide v.7.0.